

Signal Processing on Graphs: Modeling (Causal) Relations in Big Data

Jonathan Mei and José M. F. Moura

Abstract

Many *big data* applications collect a large number of time series, for example, the financial data of companies quoted in a stock exchange, the health care data of all patients that visit the emergency room of a hospital, or the temperature sequences continuously measured by weather stations across the US. A first task in the analytics of these data is to derive a low dimensional representation, a graph or discrete manifold, that describes well the *inter*relations among the time series and their *intrare*lations across time. This paper presents a computationally tractable algorithm for estimating this graph structure from the available data. This graph is directed and weighted, possibly representing *causation* relations, not just correlations as in most existing approaches in the literature. The algorithm is demonstrated on random graph and real network time series datasets, and its performance is compared to that of related methods. The adjacency matrices estimated with the new method are close to the true graph in the simulated data and consistent with prior physical knowledge in the real dataset tested.

Keywords: Graph Signal Processing, Graph Structure, Adjacency Matrix, Network, Time Series, Big Data, Causal

The authors are with the Department of Electrical and Computer Engineering, Carnegie Mellon University, Pittsburgh, PA 15213, USA. ph: (412)268-6341; fax: (412)268-3890; e-mails: [jmei,moura]@ece.cmu.edu.

This work was partially funded by AFOSR grant FA95501210087.

I. INTRODUCTION

There is an explosion of data, generated, measured, and stored at very fast rates in many disciplines, from finance and social media to geology and biology. Much of this *Big Data* takes the form of simultaneous, long running time series. Examples, among many others, include protein-to-protein interactions in organisms, patients records in health care, customers consumptions in (power, water, natural gas) utility companies, cell phone usage for wireless service providers, companies financial data, social interactions among individuals in a population. The internet-of-things (IoT) is an imminent source of ever increasing large collection of time series. The diversity and *unstructured* nature of Big Data challenges our ability to derive models from first principles; in alternative, because data is abundant, it is of great significance to develop methodologies that, in collaboration with domain experts, assist extracting low-dimensional representations for the data. Networks or graphs are becoming prevalent as models to describe data relationships. These low-dimensional graph data representations are then used for further analytics, for example, to compute statistics, make inferences, perform signal processing tasks [1], [2], [3], or quantify how topology influences diffusion in networks of agents [4].

In many problems, the first issue to address is inferring the unknown relations between entities from the data [5]. Early work include dimensionality reduction approaches such as [6], [7]. This paper focus on this problem for time-series data, estimating the network structure in the form of a possibly directed, weighted adjacency matrix \mathbf{A} . Current work on estimating network structure largely associates graph structure with assuming that the process supported by the graph is Markov [8]. Our work instead associates the graph with causal network effects, drawing inspiration from the Discrete Signal Processing on Graphs (DSP_G) framework [3], [9].

We first provide a brief overview of the concepts and notations underlying the DSP_G theory in section II. Then we introduce related prior work in section III and our new network process in section IV. Next, we present algorithms to infer the network structure from data generated by such processes in section V. Finally, we show simulation results in section VII and conclude the paper in section VIII.

II. DISCRETE SIGNAL PROCESSING ON GRAPHS

DSP_G provides a framework with which to analyze data with N elements for which relational information between elements is known. We follow [3], [9] in this brief review.

A. Graph Signals

Consider a graph $G = (\mathcal{V}, \mathbf{A})$ where the vertex set $\mathcal{V} = \{v_0, \dots, v_{N-1}\}$ and \mathbf{A} is the weighted adjacency matrix of the graph. Each data element corresponds to a node v_n and weight $\mathbf{A}_{n,m}$ is assigned to a directed edge from v_m to v_n . A graph signal is defined as a map

$$\mathbf{x} : \mathcal{V} \rightarrow \mathbb{C}$$

$$v_n \mapsto x_n$$

Since signals are isomorphic to complex vectors with N elements, we can write graph signals as N length vectors supported on \mathcal{V} ,

$$\mathbf{x} = (x_0 \ x_1 \ \dots \ x_{N-1})^T \in \mathbb{C}^N$$

B. Graph Filters

A graph filter is a system $\mathbf{H}(\cdot)$ that takes a graph signal \mathbf{x} as input and outputs another graph signal $\tilde{\mathbf{x}} = \mathbf{H}(\mathbf{x})$. A basic nontrivial graph filter on graph $G = (\mathcal{V}, \mathbf{A})$ called the graph shift is a local operation given by the product of the input signal with the adjacency matrix $\tilde{\mathbf{x}} = \mathbf{A}\mathbf{x}$. Assuming shift invariance, graph filters in DSP_G are matrix polynomials of the form

$$h(\mathbf{A}) = h_0\mathbf{I} + h_1\mathbf{A} + \dots + h_L\mathbf{A}^L$$

The output of the filter is $\tilde{\mathbf{x}} = \mathbf{H}(\mathbf{x}) = h(\mathbf{A})\mathbf{x}$. Note that graph filters are linear shift-invariant filters. For a linear combination of graph signal inputs they produce the same linear combination of graph signal outputs, and consecutive application of multiple graph filters does not depend on the order of application (i.e., graph filters commute). Graph filters also have at most $L \leq N_{\mathbf{A}}$ taps h_ℓ , where $N_{\mathbf{A}} = \deg m_{\mathbf{A}}(z)$ is the degree of the minimal polynomial $m_{\mathbf{A}}(z)$ of \mathbf{A} .

III. RELATION TO PRIOR WORK

Here we describe previous models and methods used to estimate graph structure, noting the similarities and distinctions with the method presented in this paper. In particular, in section III-A we consider sparse Gaussian graphical model selection, and in section III-B we consider sparse vector autoregression.

A. Sparse Graphical Model Selection

Sparse inverse covariance estimation [10], [11], [8] combines the Markov property with the assumption of Gaussianity to learn a graph structure describing symmetric relations between the variables. A typical formulation of sparse inverse covariance estimation is Graphical Lasso [10]. Suppose the data matrix representing all the observations is given,

$$\mathbf{X} = (\mathbf{x}[0] \ \mathbf{x}[1] \ \dots \ \mathbf{x}[K-1]) \in \mathbb{R}^{N \times K} \quad (1)$$

In this problem, the data is assumed to be Gaussian, i.e. each $\mathbf{x}[i] \sim \mathcal{N}(\mathbf{0}, \Sigma)$, independent, identically distributed, and an estimate for $\Theta = \Sigma^{-1}$ is desired. The regularized likelihood function is maximized, leading to the optimization,

$$\hat{\Theta} = \underset{\Theta}{\operatorname{argmin}} \operatorname{tr}(S\Theta) - \log |\Theta| + \lambda \|\Theta\|_1 \quad (2)$$

where $S = \frac{1}{K} \mathbf{X} \mathbf{X}^T$ is the sample covariance matrix and $\|\Theta\|_1 = \sum_{i,j} |\Theta_{ij}|$.

For independent observations, the inverse covariance matrix corresponds to instantaneous second-order relations that can be useful for inference using graphical models. However, given time series data generated from a sparse graph process, the inverse covariance matrix Θ can actually reflect higher order effects and be significantly less sparse than the graph underlying the process. For example, if a process is described by the dynamic equation with sparse state evolution matrix \mathbf{A} and $\|\mathbf{A}\|_2 \leq 1$,

$$\mathbf{x}[k] = \mathbf{A}\mathbf{x}[k-1] + \mathbf{w}[k]$$

where $\mathbf{w}[i]$ is a random noise process that is generated independently from $\mathbf{w}[j]$ for all $i \neq j$, then

$$\begin{aligned} \Sigma &= \mathbb{E} [\mathbf{x}[k]\mathbf{x}[k]^T] = \sum_{i=0}^{\infty} \mathbf{A}^i \mathbf{R} (\mathbf{A}^T)^i \\ \Rightarrow \Theta &= \left(\sum_{i=0}^{\infty} \mathbf{A}^i \mathbf{R} (\mathbf{A}^T)^i \right)^{-1} \end{aligned}$$

Even though the process can be described by sparse matrix \mathbf{A} , the true value of Θ represents powers of \mathbf{A} and need not be as sparse as \mathbf{A} . In addition, \mathbf{A} may not be symmetric, i.e. the underlying graph may be directed, while Θ is symmetric and the corresponding graph is undirected.

B. Sparse Vector Autoregressive Estimation

For time series data, instead of estimating inverse covariance structure, sparse vector autoregressive (SVAR) estimation [12], [13], [14] recovers matrix coefficients for multivariate processes. This SVA model assumes the time series at each node are conditionally independent from each other according to a Markov Random Field (MRF) with adjacency structure given by $\mathbf{A}' \in \{0, 1\}^{N \times N}$. This problem assumes given data matrix of the form in equation (1) that is generated by the dynamic equation with sparse evolution matrices $\{\mathbf{A}^{(i)}\}$,

$$\mathbf{x}[k] = \sum_{i=1}^M \mathbf{A}^{(i)} \mathbf{x}[k-i] + \mathbf{w}[k]$$

where $\mathbf{w}[i]$ is a random noise process that is generated independently from $\mathbf{w}[j]$ for all times $i \neq j$, and $\mathbf{A}^{(i)}$ all have the same sparse structure. That is, $\mathbf{A}'_{ij} = 0 \Rightarrow \mathbf{A}^{(k)}_{ij} = 0$ for all k . Then SVA solves the optimization,

$$\begin{aligned} \{\widehat{\mathbf{A}}^{(i)}\} = \operatorname{argmin}_{\{\mathbf{A}^{(i)}\}} \frac{1}{2} \sum_{k=M}^{K-1} \left\| \mathbf{x}[k] - \sum_{i=1}^M \mathbf{A}^{(i)} \mathbf{x}[k-i] \right\|_2^2 \\ + \lambda \sum_{i,j} \|\mathbf{a}_{ij}\|_2 \end{aligned} \quad (3)$$

where $\mathbf{a}_{ij} = \begin{pmatrix} A_{ij}^{(1)} & \dots & A_{ij}^{(M)} \end{pmatrix}^T$ and the term $\|\mathbf{a}_{ij}\|_2$ promotes sparsity of the (i, j) -th entry of each $\mathbf{A}^{(i)}$ matrix simultaneously and thus also sparsity of \mathbf{A}' . This optimization can be solved using Group Lasso [10]. SVA estimation methods estimate multiple weighted graphs $\mathbf{A}^{(i)}$ that can be used to estimate the sparsity structure \mathbf{A}' .

This set of $\{\mathbf{A}^{(i)}\}$ can be more challenging to interpret and analyze than a single weighted adjacency matrix, but using the single unweighted matrix \mathbf{A}' discards temporal and weight information. Also, it is not clear that the Markov property between nodes is a valid assumption for various applications described by graph processes. In contrast, our model is defined by a single weighted graph \mathbf{A} , but the corresponding time filter coefficients (introduced in section IV-A) are modeled as graph filters, which allows describing processes that are non-Markov on the graph.

IV. GRAPH PROCESSES

Section IV-A presents our new model for graph processes, section IV-B relates it to discretization of partial differential equations, and section IV-C relates the approach to graph signal processing frameworks.

A. Causal Graph Process

Consider $x_n[k]$, a discrete time series on node v_n in graph $G = (\mathcal{V}, \mathbf{A})$, where n indexes the nodes of the graph and k indexes the time samples. Let N be the total number of nodes and K be the total number of time samples, and

$$\mathbf{x}[k] = (x_0[k] \ x_1[k] \ \dots \ x_{N-1}[k])^T \in \mathbb{C}^N$$

represents the graph signal at time sample k .

We consider a Causal Graph Process (CGP) to be a discrete time series $\mathbf{x}[k]$ on a graph $G = (\mathcal{V}, \mathbf{A})$ of the following form,

$$\begin{aligned} \mathbf{x}[k] &= \mathbf{w}[k] + \sum_{i=1}^M P_i(\mathbf{A}) \mathbf{x}[k-i] \\ &= \mathbf{w}[k] + \sum_{i=1}^M \left(\sum_{j=0}^i c_{ij} \mathbf{A}^j \right) \mathbf{x}[k-i] \\ &= \mathbf{w}[k] + (c_{10} \mathbf{I} + c_{11} \mathbf{A}) \mathbf{x}[k-1] \\ &\quad + (c_{20} \mathbf{I} + c_{21} \mathbf{A} + c_{22} \mathbf{A}^2) \mathbf{x}[k-2] + \dots \\ &\quad + (c_{M0} \mathbf{I} + \dots + c_{MM} \mathbf{A}^M) \mathbf{x}[k-M] \end{aligned} \tag{4}$$

where $P_i(\mathbf{A})$ is a matrix polynomial in \mathbf{A} , $\mathbf{w}[k]$ is statistical noise, c_{ij} are scalar polynomial coefficients, and

$$\mathbf{c} = (c_{10} \ c_{11} \ \dots \ c_{ij} \ \dots \ c_{MM})^T$$

is a vector collecting all the c_{ij} 's.

Note that this model does *not* assume Markovianity on nodes and their neighbors. It instead asserts that the signal on a node at the current time is affected through network effects by signals on other nodes at past times. Matrix polynomial $P_i(\mathbf{A})$ is at most of order $\min(i, N_{\mathbf{A}})$, reflecting that $\mathbf{x}[k]$ cannot be influenced by more than i -th order network effects from i time steps ago and in addition is limited by $N_{\mathbf{A}}$, the degree of the minimum polynomial of \mathbf{A} . Typically, we take the model order $M \ll N_{\mathbf{A}}$.

B. Partial Differential Equations

We provide an intuitive motivation for the CGP model of (4). Now consider $x_n(t)$, a continuous time signal on node v_n in graph $G = (\mathcal{V}, \mathbf{A})$, where n indexes the nodes of the graph and t indexes the time samples. Let N be the total number of nodes and

$$\mathbf{x}(t) = \begin{pmatrix} x_0(t) & x_1(t) & \dots & x_{N-1}(t) \end{pmatrix}^T \in \mathbb{C}^N$$

represents the graph signal at time t .

Suppose $\mathbf{x}(t)$ is described by the M -th order differential equation,

$$\begin{aligned} \mathbf{x}^{(M)}(t) &= \sum_{i=1}^M P_i(\mathbf{B}) \mathbf{x}^{(M-i)}(t) \\ &= \sum_{i=1}^M \left(\sum_{j=0}^i c_{ij} \mathbf{B}^j \right) \mathbf{x}^{(M-i)}(t) \\ &= (c_{10}\mathbf{I} + c_{11}\mathbf{B}) \mathbf{x}^{(M-1)}(t) \\ &\quad + (c_{20}\mathbf{I} + c_{21}\mathbf{B} + c_{22}\mathbf{B}^2) \mathbf{x}^{(M-2)}(t) + \dots \\ &\quad + (c_{M0}\mathbf{I} + \dots + c_{MM}\mathbf{B}^M) x(t) \end{aligned} \tag{5}$$

where $\mathbf{x}^{(i)}(t) = \frac{\partial^i \mathbf{x}(t)}{\partial t^i}$ and \mathbf{B} is a matrix approximating a first order differential operator in the space of \mathbf{x} .

Discretizing (5) with time step size Δ ,

$$\begin{aligned} &\sum_{i=0}^M \frac{(-1)^i}{\Delta^M} \binom{M}{i} \mathbf{x}[k-i] \\ &= (c_{10}\mathbf{I} + c_{11}\mathbf{A}) \sum_{i=0}^{M-1} \frac{(-1)^i}{\Delta^{M-1}} \binom{M-1}{i} \mathbf{x}[k-1-i] \\ &\quad + \dots + (c_{M0}\mathbf{I} + \dots + c_{MM}\mathbf{A}^M) \mathbf{x}[k-M] \end{aligned} \tag{6}$$

where $\mathbf{A} = e^{\Delta \mathbf{B}}$ is a matrix operation approximating the temporal discretization of the \mathbf{B} operator at the graph nodes, and $\mathbf{x}[k] = \mathbf{x}(t)|_{t=k\Delta}$. Grouping terms containing $\mathbf{x}[k-i]$ to simplify (6) and renaming constants, we arrive at our model from (4).

C. Graph Signal Processing for Big Data

The $P_i(\mathbf{A})$ from equation (4) can be seen in the DSP_G framework as a causal graph filter. This allows us to naturally fit this model into the graph signal processing for big data framework, in

which true graphs for large datasets can be expressed or approximated by graph products, which are sums of products, for example Kronecker products [15],

$$\mathbf{A}_0 = \sum_{i=1}^M \mathbf{A}_{ti} \otimes \mathbf{A}_{si}$$

in which \mathbf{A}_{ti} are jointly diagonalized by one eigenvector basis and \mathbf{A}_{si} are jointly diagonalized by a second eigenvector basis,

$$\mathbf{A}_{ti} = \mathbf{V}_t \mathbf{\Lambda}_{ti} \mathbf{V}_t^{-1}$$

$$\mathbf{A}_{si} = \mathbf{V}_s \mathbf{\Lambda}_{si} \mathbf{V}_s^{-1}$$

This allows the eigendecomposition of \mathbf{A} to be found in terms of simpler eigendecompositions of smaller matrices \mathbf{A}_{si} and \mathbf{A}_{ti} ,

$$\mathbf{A}_0 = \mathbf{V} \mathbf{\Lambda} \mathbf{V}^{-1} = \sum_{i=1}^M (\mathbf{V}_t \otimes \mathbf{V}_s) (\mathbf{\Lambda}_{ti} \otimes \mathbf{\Lambda}_{si}) (\mathbf{V}_t^{-1} \otimes \mathbf{V}_s^{-1})$$

For our time-series process, we know that the form of one set of adjacency matrices is powers of the cyclic shift matrix $\mathbf{A}_{ti} = (\mathbf{C}^i)^T$, where

$$\mathbf{C} = \begin{pmatrix} & & & 1 \\ 1 & & & \\ & \ddots & & \\ & & & 1 \end{pmatrix},$$

(only nonzero elements shown) representing the directed cycle graph and $\mathbf{A}_{si} = P_i(\mathbf{A})$. The diagonalizing matrix for the \mathbf{A}_{ti} is the Discrete Fourier Transform (DFT) matrix.

If this cyclic temporal structure is used to represent (4), we arrive at

$$\begin{aligned} \mathbf{X} &= \sum_{i=1}^M P_i(\mathbf{A}) \mathbf{X} \mathbf{C}^i + \mathbf{W} \\ \Rightarrow \text{vec}(\mathbf{X}) &= \sum_{i=1}^M ((\mathbf{C}^i)^T \otimes P_i(\mathbf{A})) \text{vec}(\mathbf{X}) + \text{vec}(\mathbf{W}) \\ &= \mathbf{A}_0 \text{vec}(\mathbf{X}) + \text{vec}(\mathbf{W}) \end{aligned} \tag{7}$$

where \mathbf{X} is the data matrix defined as in (1) and \mathbf{W} is an error matrix. This results in a slightly different model than (4). However, for the remainder of this paper, we will use (4) to represent and estimate $P_i(\mathbf{A})$ from observed time series data.

V. ESTIMATING ADJACENCY MATRICES

Given a time series $\mathbf{x}(t)$ on graph $G = (\mathcal{V}, \mathbf{A})$ with *unknown* \mathbf{A} , we wish to estimate the adjacency matrix \mathbf{A} . A first approach to its estimation can be formulated as the following optimization problem,

$$\begin{aligned} (\mathbf{A}, \mathbf{c}) = \operatorname{argmin}_{\mathbf{A}, \mathbf{c}} & \frac{1}{2} \sum_{k=M}^{K-1} \left\| \mathbf{x}[k] - \sum_{i=1}^M P_i(\mathbf{A}) \mathbf{x}[k-i] \right\|_2^2 \\ & + \lambda_1 \|\operatorname{vec}(\mathbf{A})\|_1 + \lambda_2 \|\mathbf{c}\|_1 \end{aligned} \quad (8)$$

where

$$\mathbf{X} = (\mathbf{x}[0] \ \mathbf{x}[1] \ \dots \ \mathbf{x}[K-1])$$

represents all the data and $\operatorname{vec}(\mathbf{A})$ represents the matrix \mathbf{A} seen as a long vector. Assuming that $c_{11} \neq 0$, then without further loss of generality we can fix $c_{10} = 0$ and $c_{11} = 1$ to ensure that \mathbf{A} is uniquely recoverable.

In equation (8), the first term in the right hand side models $\mathbf{x}[k]$ by the CGP model in section IV-A, the regularizing term $\lambda_1 \|\operatorname{vec}(\mathbf{A})\|_1$ promotes sparsity of the estimated adjacency matrix, and the term $\lambda_2 \|\mathbf{c}\|_1$ also promotes sparsity in the matrix polynomial coefficients. Unfortunately, the matrix polynomial in the first term makes this problem highly nonconvex. That is, using a convex optimization based approach to solve (8) directly may result in finding a matrix $\hat{\mathbf{A}}$ and coefficients $\hat{\mathbf{c}}$ minimizing the objective function locally, finding a solution that is not near to the true globally minimizing matrix \mathbf{A} and coefficients \mathbf{c} .

Instead, our approach here is to break this estimation down into three separate, more tractable steps:

- 1) Solve for $\mathbf{R}_i = P_i(\mathbf{A})$
- 2) Recover structure of \mathbf{A}
- 3) Estimate c_{ij}

A. Solving for $P_i(\mathbf{A})$

As previously stated, the graph filters $P_i(\mathbf{A})$ are polynomials of \mathbf{A} and are thus shift-invariant and must mutually commute. Then their commutator

$$[P_i(\mathbf{A}), P_j(\mathbf{A})] = P_i(\mathbf{A})P_j(\mathbf{A}) - P_j(\mathbf{A})P_i(\mathbf{A}) = 0 \quad \forall i, j$$

Let $\mathbf{R} = (\mathbf{R}_1, \dots, \mathbf{R}_M)$; $\hat{\mathbf{R}}_i$ is the estimate of $P_i(\mathbf{A})$. This leads to the optimization problem,

$$\begin{aligned} \widehat{\mathbf{R}} = & \underset{\mathbf{R}}{\operatorname{argmin}} \frac{1}{2} \sum_{k=M}^{K-1} \left\| \mathbf{x}[k] - \sum_{i=1}^M \mathbf{R}_i \mathbf{x}[k-i] \right\|_2^2 \\ & + \lambda_1 \|\operatorname{vec}(\mathbf{R}_1)\|_1 + \lambda_2 \sum_{i \neq j} \|\mathbf{R}_i \mathbf{R}_j\|_F^2 \end{aligned} \quad (9)$$

While this is still a non-convex problem, it is multi-convex. That is, when $\mathbf{R}_{-i} = \{\mathbf{R}_j : j \neq i\}$ (all \mathbf{R}_j except for \mathbf{R}_i) are held constant, the optimization is convex in \mathbf{R}_i . This naturally leads to block coordinate descent as a solution,

$$\begin{aligned} \widehat{\mathbf{R}}_i = & \underset{\mathbf{R}_i}{\operatorname{argmin}} \frac{1}{2} \sum_{k=M}^{K-1} \left\| \mathbf{x}[k] - \sum_{i=1}^M \mathbf{R}_i \mathbf{x}[k-i] \right\|_2^2 \\ & + \lambda_1 \|\operatorname{vec}(\mathbf{R}_1)\|_1 + \lambda_2 \sum_{j \neq i} \|\mathbf{R}_i \mathbf{R}_j\|_F^2 \end{aligned} \quad (10)$$

Each of these sub-problems for estimating \mathbf{R}_i in a single sweep of estimating \mathbf{R} is formulated as an ℓ_1 -regularized least-squares problem that can be solved using standard methods [16].

B. Recovering \mathbf{A}

After obtaining estimates $\widehat{\mathbf{R}}_i$, we find an estimate for \mathbf{A} . One approach is to take $\widehat{\mathbf{A}} = \widehat{\mathbf{R}}_1$. This appears to ignore the information from the remaining $\widehat{\mathbf{R}}_i$. However, the information has already been incorporated during the iterations when solving for $\widehat{\mathbf{R}}$, especially if we begin one new sweep to estimate \mathbf{R}_1 using (10) with $i = 1$. A second approach is also possible, explicitly using all the $\widehat{\mathbf{R}}_i$ together to find \mathbf{A} ,

$$\begin{aligned} \widehat{\mathbf{A}} = & \underset{\mathbf{A}}{\operatorname{argmin}} \left\| \widehat{\mathbf{R}}_1 - \mathbf{A} \right\|_2^2 + \lambda_1 \|\operatorname{vec}(\mathbf{A})\|_1 \\ & + \lambda_2 \sum_{i=2}^M \left\| [\mathbf{A}, \widehat{\mathbf{R}}_i] \right\|_F^2 \end{aligned} \quad (11)$$

This can be seen as similar to running one additional step further in the block coordinate descent to find $\widehat{\mathbf{R}}_1$ except that this approach does not explicitly use the data.

C. Estimating \mathbf{c}

We can estimate c_{ij} in one of two ways: we can estimate \mathbf{c} either from $\widehat{\mathbf{A}}$ and $\widehat{\mathbf{R}}_i$ or from $\widehat{\mathbf{A}}$ and the data \mathbf{X} .

To estimate c_{ij} from $\widehat{\mathbf{A}}$ and $\widehat{\mathbf{R}}$, we set up the optimization,

$$\widehat{\mathbf{c}}_i = \operatorname{argmin}_{\mathbf{c}_i} \frac{1}{2} \left\| \widehat{\mathbf{R}}_i - \mathbf{Q}_i \mathbf{c}_i \right\|_2^2 + \lambda_3 \|\mathbf{c}_i\|_1 \quad (12)$$

where

$$\begin{aligned} \mathbf{Q}_i &= \begin{pmatrix} \operatorname{vec}(\mathbf{I}) & \operatorname{vec}(\widehat{\mathbf{A}}) & \dots & \operatorname{vec}(\widehat{\mathbf{A}}^i) \end{pmatrix}, \\ \mathbf{c}_i &= (c_{i0} \ c_{i1} \ \dots \ c_{ii})^T \end{aligned}$$

Alternatively, to estimate c_{ij} from $\widehat{\mathbf{A}}$ and the data \mathbf{X} , we can use the optimization,

$$\widehat{\mathbf{c}} = \operatorname{argmin}_{\mathbf{c}} \frac{1}{2} \|\mathbf{Y} - \mathbf{B}\mathbf{c}\|_F^2 + \lambda_3 \|\mathbf{c}\|_1 \quad (13)$$

where $\mathbf{Y} = \operatorname{vec}(\mathbf{X}_M)$,

$$\begin{aligned} \mathbf{B} &= \left(\operatorname{vec}(\mathbf{X}_{M-1}) \dots \operatorname{vec}(\widehat{\mathbf{A}}^i \mathbf{X}_{M-j}) \dots \operatorname{vec}(\widehat{\mathbf{A}}^M \mathbf{X}_0) \right), \\ \mathbf{X}_m &= \begin{pmatrix} \mathbf{x}[m] & \mathbf{x}[m+1] & \dots & \mathbf{x}[m+K-M-1] \end{pmatrix}, \end{aligned}$$

which can also be solved using standard ℓ_1 -regularized least squares methods.

D. General Estimation

The methods discussed so far can be interpreted as assuming that 1) the process is a linear autoregressive process driven by white Gaussian noise and 2) the parameters \mathbf{A} and \mathbf{c} a priori follow Laplace distributions. The objective function in (8) approximately corresponds to the log posterior density and its solution to an approximate maximum a posteriori (MAP) estimate.

This framework can be extended to estimate more general autoregressive processes, such as those with a non-Gaussian noise model and certain forms of nonlinear dependence of the current state on past values of the state. We formulate the general optimization

$$\begin{aligned} (\mathbf{A}, \mathbf{c}) &= \operatorname{argmin}_{\mathbf{A}, \mathbf{c}} f(\mathbf{X}, P_1(\mathbf{A}), \dots, P_M(\mathbf{A})) \\ &\quad + g_1(\mathbf{A}) + g_2(\mathbf{c}) \end{aligned} \quad (14)$$

where $f(\cdot, \dots, \cdot)$ is a loss function that can correspond to a log-likelihood function dictated by the noise model, and $g_1(\cdot)$ and $g_2(\cdot)$ are regularization functions (usually convex norms) that can correspond to log-prior distributions imposed on the parameters and are dictated by modeling assumptions. Again, the matrix polynomials $P_i(\mathbf{A})$ introduce nonconvexity, so similarly as before, we can separate the estimation into three steps to reduce complexity.

We next generalize equation (10) used to find \mathbf{R}_i as estimates of $P_i(\mathbf{A})$ with the optimization

$$\begin{aligned}\widehat{\mathbf{R}}_i = \operatorname{argmin}_{\mathbf{R}_i} f_i(\mathbf{X}, \mathbf{R}_i) + g_{1i}(\mathbf{R}_i) \\ + g_{2i}([\mathbf{R}_i, \widehat{\mathbf{R}}_1], \dots, [\mathbf{R}_i, \widehat{\mathbf{R}}_M])\end{aligned}\tag{15}$$

where $f_i(\cdot, \cdot)$ is the part of the objective function that depends on $P_i(\mathbf{A})$ when the other \mathbf{R}_{-i} are fixed, the term $g_{1i}(\cdot)$ regularizes the estimated matrix polynomial, and the term $g_{2i}(\cdot, \dots, \cdot)$ promotes commutativity of the matrix polynomials.

Next, we can again take $\mathbf{A} = \mathbf{R}_1$, or we can reformulate equation (11)

$$\widehat{\mathbf{A}} = \operatorname{argmin}_{\mathbf{A}} f(\widehat{\mathbf{R}}_1, \mathbf{A}) + g_1(\mathbf{A}) + g_2(\mathbf{A}, \widehat{\mathbf{R}}_{-1})\tag{16}$$

where $f(\cdot)$ is some loss function, $g_1(\cdot)$ regularizes the estimated adjacency matrix, and $g_2(\mathbf{A}, \widehat{\mathbf{R}}_{-1})$ enforces commutativity of the adjacency matrix with the other matrix polynomials.

We can generalize (12) as

$$\widehat{\mathbf{c}}_i = \operatorname{argmin}_{\mathbf{c}_i} f\left(\widehat{\mathbf{R}}_i, \mathbf{Q}_i \mathbf{c}_i\right) + g(\mathbf{c}_i)\tag{17}$$

where $f(\cdot)$ is the objective function, and $g(\cdot)$ is a regularizing function on the matrix polynomial coefficients, and \mathbf{Q}_i is defined as in section V-C; and lastly generalize (13) as

$$\widehat{\mathbf{c}} = \operatorname{argmin}_{\mathbf{c}} f(\mathbf{Y}, \mathbf{B} \mathbf{c}) + g(\mathbf{c})\tag{18}$$

where $f(\cdot)$ and $g(\cdot)$ are the same functions as above in (17), and \mathbf{Y} and \mathbf{B} are defined as in section V-C.

E. Extension of Estimation

In sections V-A-V-C, we have outlined a 3-step algorithm to obtain estimates $\widehat{\mathbf{A}}$ and $\widehat{\mathbf{c}}$ for the adjacency matrix and filter coefficients as a more efficient and well-behaved alternative to directly using (14).

We call this 3-step procedure the basic algorithm, which is outlined in algorithm 1. Superscripts denote the iteration number, $\widehat{\mathbf{R}}_{<i}^{(t)}$ denotes $\{\widehat{\mathbf{R}}_j^{(t)} : j < i\}$ and likewise $\widehat{\mathbf{R}}_{>i}^{(t)}$ denotes $\{\widehat{\mathbf{R}}_j^{(t)} : j > i\}$, and T is the final iteration performed before convergence of $\widehat{\mathbf{R}}$ is determined or a preset maximum iteration count is exceeded.

As an extension of the basic algorithm, we can also choose the estimated matrix $\widehat{\mathbf{A}}$ and filter coefficients $\widehat{\mathbf{c}}$ to initialize the direct approach of using (14). Starting from these initial points, we may find better local minima than with initializations at $\mathbf{A} = \mathbf{0}$ and $\mathbf{c} = \mathbf{0}$ or at random points. We call this procedure the extended algorithm, summarized in algorithm 2.

Algorithm 1 Basic estimation algorithm

Initialize, $t = 0$, $\widehat{\mathbf{R}}^{(t)} = 0$

while $\widehat{\mathbf{R}}^{(t)}$ not converged **do**

for $i = 1 : M$ **do**

 Find $\widehat{\mathbf{R}}_i^{(t)}$ with fixed $\widehat{\mathbf{R}}_{<i}^{(t)}$, $\widehat{\mathbf{R}}_{>i}^{(t-1)}$ using (15).

end for

$t \leftarrow t + 1$

end while

Set $\widehat{\mathbf{A}} = \widehat{\mathbf{R}}_1^{(T)}$ or estimate $\widehat{\mathbf{A}}$ from $\widehat{\mathbf{R}}^{(T)}$ using (16).

Solve for $\widehat{\mathbf{c}}$ from \mathbf{X} , $\widehat{\mathbf{A}}$ using (17) or from \mathbf{X} , $\widehat{\mathbf{R}}$ using (18).

Algorithm 2 Extended estimation algorithm

Estimate $\mathbf{A}^{(0)}$, $\mathbf{c}^{(0)}$ using basic algorithm.

Find $\widehat{\mathbf{A}}$, $\widehat{\mathbf{c}}$ using initialization $\mathbf{A}^{(0)}$, $\mathbf{c}^{(0)}$ from (14) using convex methods.

VI. CONVERGENCE OF ESTIMATION

In this section, we discuss the convergence of both the basic and extended algorithms described above.

A. Basic Algorithm

In estimating \mathbf{A} and \mathbf{c} , the forms of the optimization problems are well studied when choosing ℓ_2 and ℓ_1 norms as loss and regularization functions, as seen in equations (11) and (13). However, using these same norms, step 1 of the algorithm is a nonconvex optimization. Hence we would like to ensure that step 1 converges.

When using block coordinate descent for general functions, neither the solution nor the objective function values are guaranteed to converge to a global or even a local minimum. However, under some mild assumptions, using block coordinate descent to estimate \mathbf{R}_i will converge. In equation (14), if we assume the objective function to be continuous and to have convex, compact level sets in each coordinate block \mathbf{R}_i (for example, if the functions for f and g are the ℓ_2 and ℓ_1 norms as in equation (8)), then the block coordinate descent will converge [17].

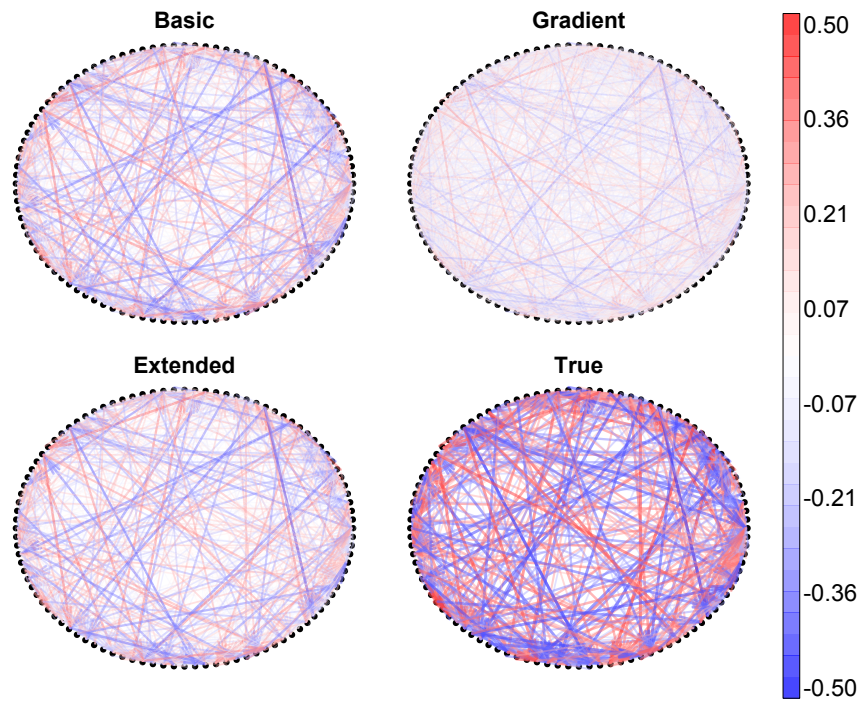
B. Extended Algorithm

Now we discuss the convergence of the extended method described in section V-E assuming that the basic algorithm has converged to an initial point $(\mathbf{A}^{(0)}, \mathbf{c}^{(0)})$ for the extended algorithm. We assume that the function $F = f + g_1 + g_2$ in equation (14) has compact level sets and is bounded below. Then an iterative convex method that produces updates of $(\mathbf{A}^{(t+1)}, \mathbf{c}^{(t+1)})$ such that $F(\mathbf{A}^{(t+1)}, \mathbf{c}^{(t+1)}) \leq F(\mathbf{A}^{(t)}, \mathbf{c}^{(t)})$ (e.g., generalized gradient descent with appropriately chosen step size) converges, possibly to a local optimum if the problem is nonconvex [18]. If the functions are the ℓ_2 and ℓ_1 norms as in equation (8), these conditions are satisfied as well.

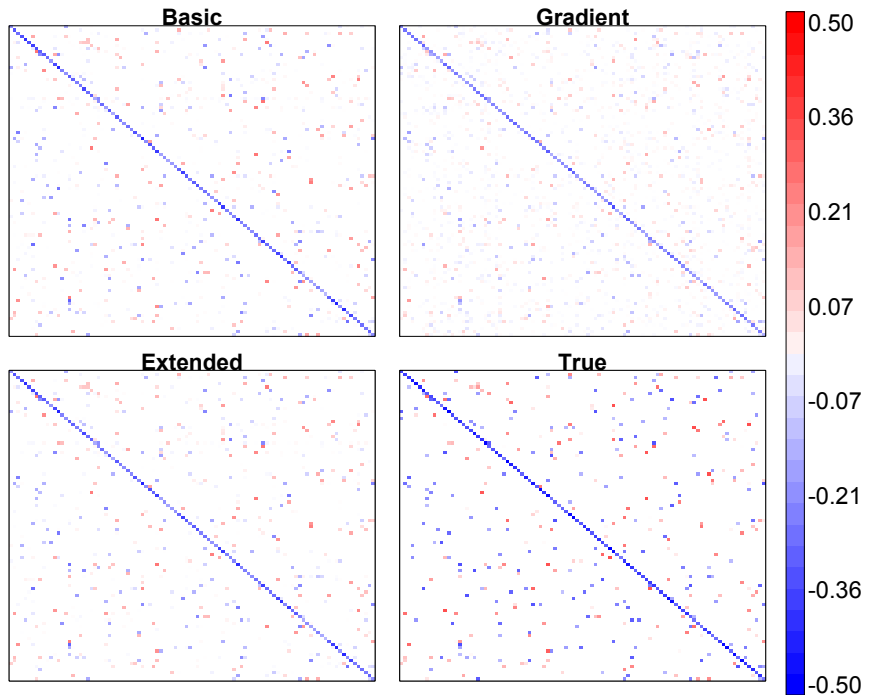
VII. EXPERIMENTS

The algorithm was tested on randomly generated examples (with varying N and K) and a real temperature sensor network dataset (with $N = 150$ and $K = 365$), sampled once per day over a year at 150 locations in the continental United States [19]. To solve the regularized least squares iterations for estimating the CGP matrices, we used Gradient Projection for Sparse Reconstruction [16]. To estimate the MRF matrices, we implemented a proximal gradient descent algorithm to estimate the SVAR matrix coefficients from 3 since the code used in [14] is not tested for larger graphs.

A. Random Network



(a) Graphs



(b) Adjacency matrices

Fig. 1. Random adjacency matrix and estimated adjacency matrices with $N = 25$, $K = 100$, $M = 3$

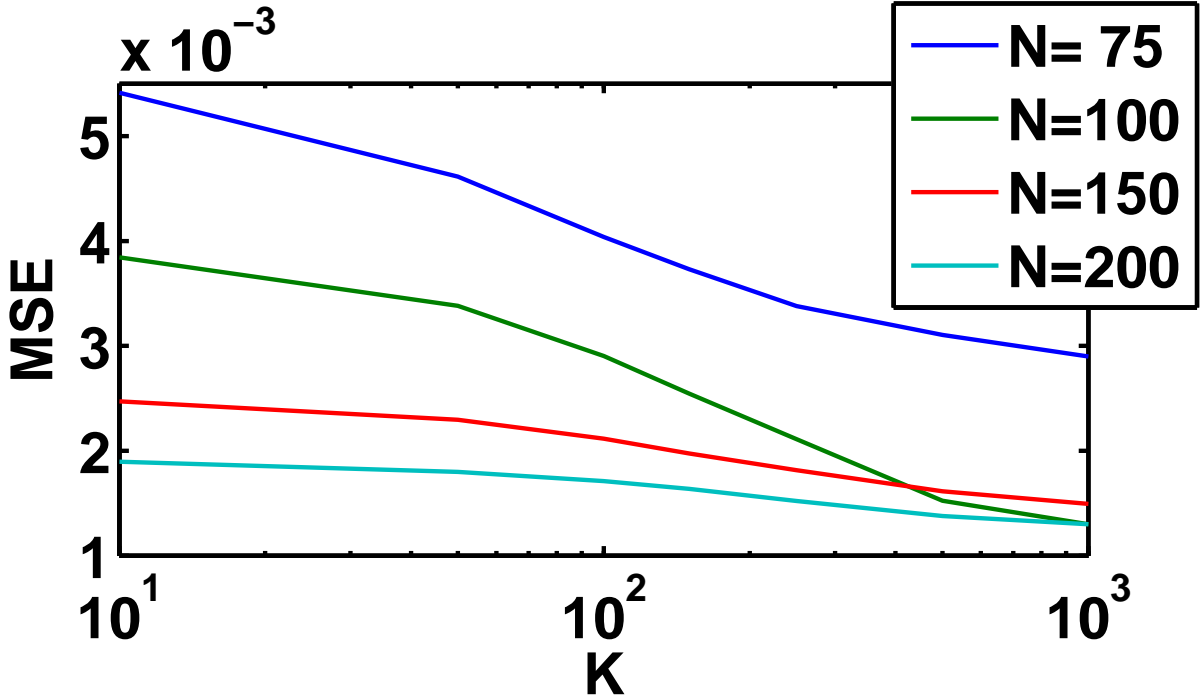


Fig. 2. MSE vs number of samples K for random graph data

The random graph dataset was generated by first creating a random sparse \mathbf{A} matrix for a graph with $N \in \{75, 100, 150, 200\}$ nodes and \mathbf{c} coefficients that corresponded to a stable system. The matrix in our simulations had each off-diagonal element independently drawn from a unit Normal $\mathcal{N}(0, 1)$ distribution and made sparse by thresholding $1.6 \leq |\mathbf{A}'_{ij}| \leq 1.8$ and then scaled to ensure stability $\mathbf{A}'' = \mathbf{A}' / (2\lambda_1(\mathbf{A}'))$ where $\lambda_1(\mathbf{A}')$ is the largest eigenvalue of \mathbf{A}' . This results in a directed, weighted Erdős-Renyi graph topology with a constant probability $p = 2(\Phi(1.8) - \Phi(1.6)) \approx 0.04$ of having an edge from node i to node j and with edge weights bounded away from 0. The diagonal elements were generated from a uniform distribution $D_{ii} \sim \mathcal{U}(-1, -0.5)$, also to ensure stability. Then the adjacency matrix was formed $\mathbf{A} = \mathbf{D} + \mathbf{A}''$. Finally, the polynomial coefficients \mathbf{c} for a process of order $M = 3$ were arbitrarily chosen to result in a stable process. The data matrix \mathbf{X} was formed by generating random initial states and zero-mean unit-covariance additive white Gaussian noise $\mathbf{w}[k]$, and computing $K \in \{10, 25, 50, 100, 250, 500, 1000\}$ samples of $\mathbf{x}[k]$ according to (4).

In figure 1(a), we see the structure of the \mathbf{A} matrix with $N = 100$ nodes used in the simulated graph to generate \mathbf{X} with $K = 100$ samples according to a CGP. We also see the structure of the $\widehat{\mathbf{A}}$ matrices estimated using the basic and extended methods, and also using the gradient method

in the extended method but initialized at the origin ($\mathbf{A}^{(0)} = 0$, $\mathbf{c}^{(0)} = 0$). While the actual graphs are directed, it is difficult to depict the direction of edges in larger graphs, so for presentation, they are shown as undirected in figure 1(a). In figure 1(b), we see the individual values of the $\widehat{\mathbf{A}}$ matrices estimated from the data \mathbf{X} . Now we note the directed nature of the graph, as the matrix is asymmetric. We see that the estimated $\widehat{\mathbf{A}}$ matrices all have almost the same support as the true \mathbf{A} matrix visually. Qualitatively, the basic method produces a less sparse solution, and the gradient method produces a lower magnitude solution, while the solution produced by the extended method is both sparse and closer in magnitude solution to the true solution. Thus we see that the extended method performs better than either the basic step or the gradient step alone. The mean squared errors (MSE's) of entries of the \mathbf{A} matrix are computed as

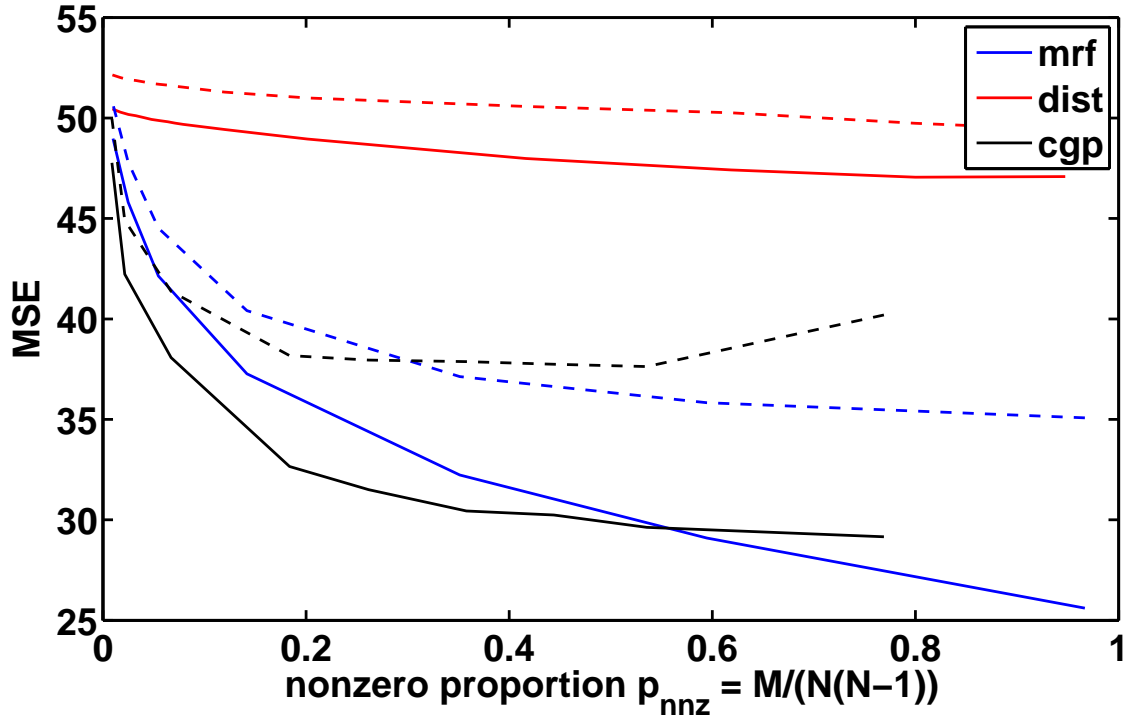
$$MSE = \frac{1}{N^2} \|\mathbf{A} - \widehat{\mathbf{A}}\|_F^2$$

The MSE's for the estimates shown in figure 1 are: 6×10^{-5} for the basic, 6×10^{-5} for the extended, and 1×10^{-3} for the gradient.

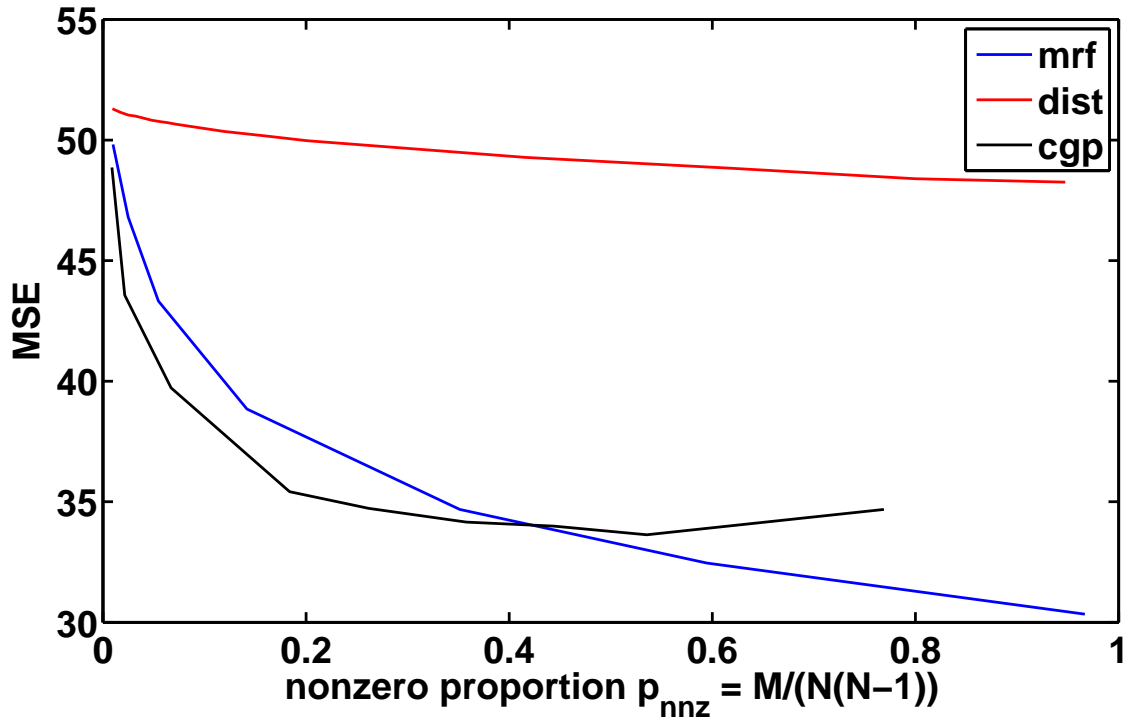
In figure 2, we see MSE for $\widehat{\mathbf{A}}$ across different numbers of time samples K on the same graph, as well as across different numbers of nodes N corresponding to distinct graphs with the same level of sparsity. The MSE is averaged over 50 Monte-Carlo simulations of the data matrix \mathbf{X} for each problem size. As expected, the MSE for each problem size decreases as the number of samples K increases. While the estimate produced by the proposed method is biased for finite K , the plot suggests that asymptotically in the number of samples K , the graph produced may still be consistent. In addition, the MSE's computed decrease with increasing N , suggesting that the total error in estimating the matrix $\|\mathbf{A} - \widehat{\mathbf{A}}\|_F^2 = o(N^2)$. The dependence of these error rates on N and K are of interest for further analysis.

B. Temperature Sensor Network

The temperature dataset is a collection of daily average temperature measurements taken over 365 days at 150 locations around the continental United States [19]. The time series \mathbf{x}_i is linearly detrended at each measurement station i to form $\widetilde{\mathbf{x}}_i$. Then the seasonally detrended time series $\bar{\mathbf{x}}_i$ are obtained by applying an ideal high-pass filter with cutoff period of 365 days to each $\widetilde{\mathbf{x}}_i$. Finally, the data matrix \mathbf{X} is formed from $\bar{\mathbf{x}}_i$

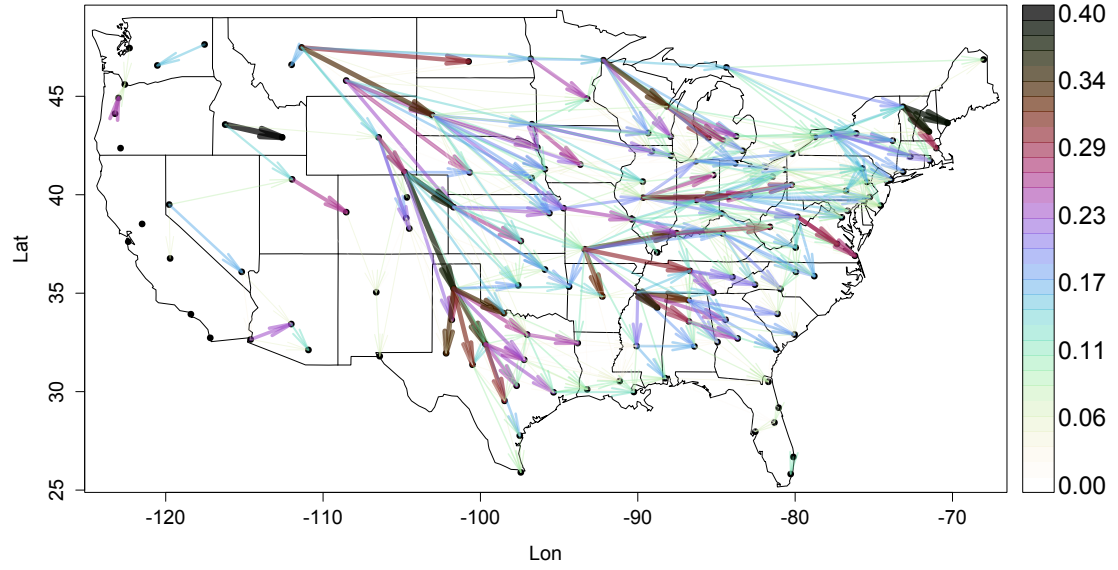


(a) Training (solid) and Testing (dashed) Errors vs Nonzeros

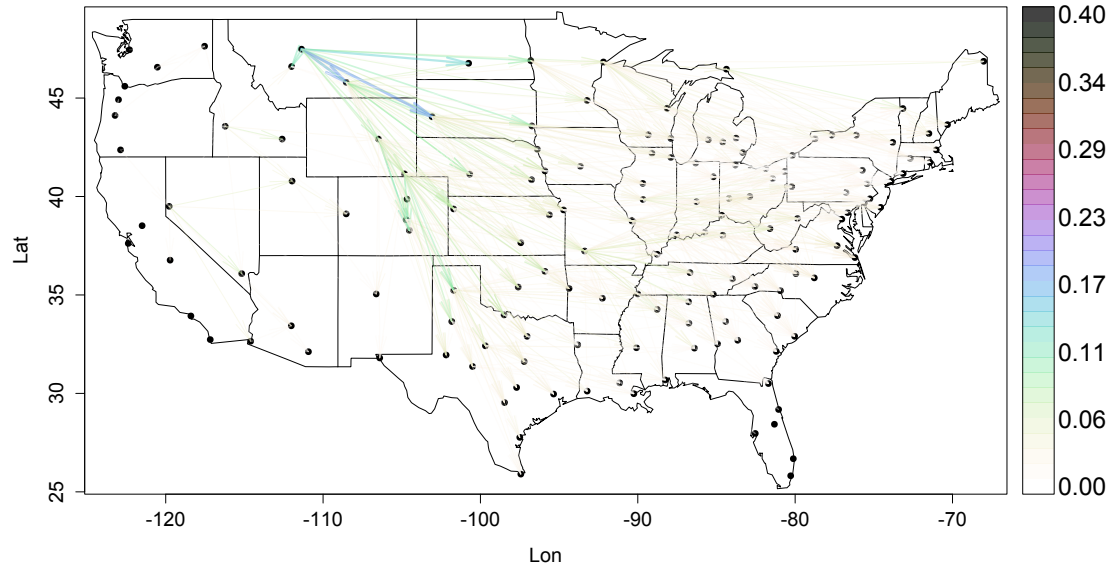


(b) Total Errors vs Nonzeros

Fig. 3. Prediction Error vs Nonzeros using order $M = 2$ model



(a) Graph estimate using CGP



(b) Graph estimate using MRF

Fig. 4. Estimated temperature graphs using order $M = 2$ model with sparsity $p_{nnz} = 0.05$

We compare the sparsity and prediction errors of using CGP and MRF models as well as

an undirected distance graph as described in [3], all on the same set of temperature data. The distance graph model uses an adjacency matrix \mathbf{A}^{dist} to model the process

$$\mathbf{x}[k] = \mathbf{w}[k] + \sum_{i=1}^M h_i(\mathbf{A}^{\text{dist}}) \mathbf{x}[k-i]$$

where $h_i(\mathbf{A}^{\text{dist}}) = \sum_{j=0}^L c_{ji}(\mathbf{A}^{\text{dist}})^j$ are polynomials of the distance matrix with elements chosen as

$$\mathbf{A}_{mn}^{\text{dist}} = \frac{e^{-d_{mn}^2}}{\sqrt{\sum_{k \in \mathcal{N}_n} e^{-d_{nk}^2} \sum_{\ell \in \mathcal{N}_m} e^{-d_{m\ell}^2}}}$$

with \mathcal{N}_n representing the neighborhood of 8 cities nearest to city n . In this model, M is taken to be fixed and the polynomial coefficients c_{ji} are to be estimated. In our experiments, we assumed $M = 2$.

We separated the data into two segments, one consisting of the even time indices and one consisting of the odd time indices. One set was used as training data and the other set was left as testing data. This way, the test and training data were both generated from almost the same process but with different daily fluctuations. In this experiment, we compute the prediction MSE as

$$MSE = \frac{1}{N(T-M)} \sum_{i=M+1}^T \|\mathbf{x}[i] - \hat{\mathbf{x}}[i]\|^2$$

Here, since we do not have the ground truth graph for this data, the experiments can be seen as corresponding to the two related tasks of compression and prediction. The training error indicates how well the estimated graph can represent or compress the entire series, while the test error indicates how well the estimated graph can predict the following time instance from past observations on new series.

In figure 3(a), we see that using a directed graph (either CGP or MRF) performs better for prediction than using an undirected distance graph in both training and testing phases. In addition, for high sparsity or low nonzeros (towards the left side of the graph with proportion of nonzeros $p_{\text{nnz}} < 0.4$), the CGP fits the data with better accuracy than the MRF model. At lower sparsity levels (towards the right side of the graph $p_{\text{nnz}} > 0.4$), the MRF model performs better than the CGP model. Figure 3(b) shows the average of test and training error labeled as total error. The same trends are present here as well, in which the CGP model outperforms the MRF model for $p_{\text{nnz}} < 0.4$. However, when the proportion of nonzeros in the adjacency matrix is above 40%,

one cannot claim that the model is truly “sparse”. Thus, when using sparse models, the CGP captures the true dynamics of the process using higher sparsity than the MRF model.

In figure 4, we compare the temperature networks estimated on the entire time series using CGP and MRF models that both have sparsity level $p_{\text{nnz}} = 0.05$. For the MRF estimate, we used the first matrix coefficient $\mathbf{A}^{(1)}$ to represent the network, although as mentioned previously there is not the interpretation of a single weighted graph being estimated using this model. The x -axis corresponds to longitude while the y -axis corresponds to latitude. We note that the network produced by the MRF at the same sparsity level has similar support to that produced by the CGP, but the magnitudes of the edges are lower. We see that the CGP model clearly picks out the predominant west-to-east direction of wind in the $x \geq -95$ portion of the country, as single points in this region are seen to predict multiple eastward points. It also shows the influence of the roughly north-northwest-to-south-southeast Rocky Mountain chain at $-110 \leq x \leq -100$. This yields easy interpretation consistent with knowledge of geographic and meteorological features.

C. Discussion

We have shown through experiments that the estimation algorithms presented are able to accurately estimate a sparse graph topology from data generated when the true model is a CGP. We have also demonstrated empirically that the CGP model can use a higher sparsity level than the MRF model to describe processes at the same levels of accuracy. For this reason, we believe that the CGP model reflects the dynamics of the process underlying the temperature sensor data more faithfully.

VIII. CONCLUSIONS

We have presented a new type of graph-based network process and a computationally tractable algorithm for estimating such causal networks. The algorithm was demonstrated on several random graphs of varying size and a real temperature sensor network dataset. The estimated adjacency matrices in the random graph examples were shown to be close to the true graph. In the real dataset, the adjacency matrices estimated using our method were consistent with prior physical knowledge and achieved lower prediction error compared to previous methods at the same sparsity level.

REFERENCES

- [1] Matthew O. Jackson, *Social and Economic Networks*, Princeton University Press, Nov. 2010.
- [2] Kevin P. Murphy, Yair Weiss, and Michael I. Jordan, “Loopy belief propagation for approximate inference: An empirical study,” in *Proceedings of the Fifteenth Conference on Uncertainty in Artificial Intelligence*, San Francisco, CA, USA, 1999, UAI’99, pp. 467–475, Morgan Kaufmann Publishers Inc.
- [3] A. Sandryhaila and J.M.F. Moura, “Discrete signal processing on graphs,” *IEEE Transactions on Signal Processing*, vol. 61, no. 7, pp. 1644–1656, Apr. 2013.
- [4] Mark Newman, *Networks: An Introduction*, Oxford University Press, Mar. 2010.
- [5] Nicolai Meinshausen and Peter Bühlmann, “High-dimensional graphs and variable selection with the lasso,” *Ann. Stat.*, vol. 34, no. 3, pp. 1436–1462, June 2006.
- [6] Sam T. Roweis and Lawrence K. Saul, “Nonlinear dimensionality reduction by locally linear embedding,” *SCIENCE*, vol. 290, pp. 2323–2326, 2000.
- [7] Joshua B. Tenenbaum, Vin de Silva, and John C. Langford, “A global geometric framework for nonlinear dimensionality reduction,” *Science*, vol. 290, no. 5500, pp. 2319–2323, 2000.
- [8] Pradeep Ravikumar, Martin J. Wainwright, Garvesh Raskutti, and Bin Yu, “High-dimensional covariance estimation by minimizing ℓ_1 -penalized log-determinant divergence,” *Electronic Journal of Statistics*, vol. 5, pp. 935–980, 2011.
- [9] A. Sandryhaila and J.M.F. Moura, “Discrete signal processing on graphs: Frequency analysis,” *IEEE Transactions on Signal Processing*, vol. 62, no. 12, pp. 3042–3054, June 2014.
- [10] Jerome Friedman, Trevor Hastie, and Robert Tibshirani, “Sparse inverse covariance estimation with the graphical lasso,” *Biostatistics*, vol. 9, no. 3, pp. 432–41, July 2008.
- [11] Venkat Chandrasekaran, Pablo A. Parrilo, and Alan S. Willsky, “Latent variable graphical model selection via convex optimization,” *The Annals of Statistics*, vol. 40, no. 4, pp. 1935–1967, Aug. 2012.
- [12] F.R. Bach and M.I. Jordan, “Learning graphical models for stationary time series,” *IEEE Transactions on Signal Processing*, vol. 52, no. 8, pp. 2189–2199, Aug. 2004.
- [13] Jitkomut Songsiri and L. Vandenberghe, “Topology selection in graphical models of autoregressive processes,” *J. Mach. Learn. Res.*, vol. 11, pp. 2671–2705, 2010.
- [14] A. Bolstad, B.D. Van Veen, and R. Nowak, “Causal network inference via group sparse regularization,” *IEEE Transactions on Signal Processing*, vol. 59, no. 6, pp. 2628–2641, June 2011.
- [15] A. Sandryhaila and J.M.F. Moura, “Big data analysis with signal processing on graphs: Representation and processing of massive data sets with irregular structure,” *IEEE Signal Processing Magazine*, vol. 31, no. 5, pp. 80–90, Sept. 2014.
- [16] M.A.T. Figueiredo, R.D. Nowak, and S.J. Wright, “Gradient projection for sparse reconstruction: Application to compressed sensing and other inverse problems,” *IEEE Journal of Selected Topics in Signal Processing*, vol. 1, no. 4, pp. 586–597, Dec. 2007.
- [17] P. Tseng, “Convergence of a block coordinate descent method for nondifferentiable minimization,” *J. Optim. Theory Appl.*, pp. 475–494, 2001.
- [18] D.P. Bertsekas, A. Nedić, and A.E. Ozdaglar, *Convex Analysis and Optimization*, Athena Scientific, 2003.
- [19] “National climactic data center,” 2011.